

Synthesis and Characterization of Bis(triaminoguanidinium) 5,5'-Dinitrimino-3,3'-azo-1H-1,2,4-triazolate – A Novel Insensitive Energetic Material

Alexander Dippold,^[a] Thomas M. Klapötke,*^[a] and Franz A. Martin^[a]

Keywords: Energetic materials; High nitrogen containing compounds; Nitamines; Sensitivities; Triazoles

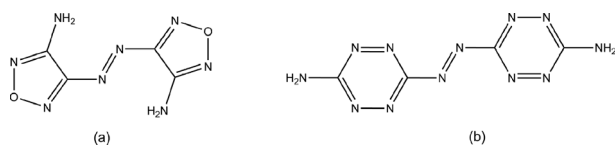
Abstract. The synthesis of 5,5'-diamino-3,3'-azo-1H-1,2,4-triazole (**3**) by reaction of 5-acetylaminoo-3-amino-1H-1,2,4-triazole (**2**) with potassium permanganate is described. The application of the very straightforward and efficient acetyl protection of 3,5-diamino-1H-1,2,4-triazole allows selective reactions of the remaining free amino group to form the azo-functionality. Compound **3** is used as starting material for the synthesis of 5,5'-dinitrimino-3,3'-azo-1H-1,2,4-triazole (**4**), which subsequently reacted with organic bases (ammonia, hydrazine, guanine, aminoguanidine, triaminoguanidine) to form the corresponding nitrogen-rich triazolate salts (**5–9**). All substances were fully characterized by IR and Raman as well as multinuclear NMR spectroscopy,

mass spectrometry, and differential scanning calorimetry. Selected compounds were additionally characterized by low temperature single-crystal X-ray diffraction measurements. The heats of formation of **4–9** were calculated by the CBS-4M method to be 647.7 (4), 401.2 (5), 700.4 (6), 398.4 (7), 676.5 (8), and 1089.2 (9) kJ·mol⁻¹. With these values as well as the experimentally determined densities several detonation parameters were calculated using both computer codes EXPL05.03 and EXPL05.04. In addition, the sensitivities of **5–9** were determined by the BAM drophammer and friction tester as well as a small scale electrical discharge device.

Introduction

In recent years, the synthesis of energetic, heterocyclic compounds has attracted an increasing amount of interest, since heterocycles generally offer a higher heat of formation, density, and oxygen balance than their carbocyclic analogues.^[1] In combination with the advantages of a high nitrogen content such as the high average two electron bond energy associated with the nitrogen–nitrogen triple bond,^[2] those compounds are of great interest for investigations. The current widely used nitro-explosives TNT, RDX, or HMX per se as well as their transformation products are toxic due to the presence of nitro (–NO₂), nitroso (–NO), or nitrito (–ONO) groups either in the explosives itself or their degradation products.^[3] The development of new energetic materials therefore focuses – besides high performance and stability – on environmentally friendly compounds. Nitrogen-rich compounds mainly generate environmentally friendly molecular nitrogen as end-product of propulsion or explosion, therefore they continue to be the focus of energetic materials research across the globe.^[4] A prominent family of compounds regarding the properties mentioned above are azole-based energetic materials, because they are generally highly endothermic compounds with relatively high densities and a high nitrogen content.^[5] Since modern high

energy density materials (HEDM) mostly derive their energy of ring or cage strain as well as of a high heat of formation, a lot of research was done on explosives containing the azo-functionality. Several heterocyclic compounds like 4,4'-diamino-3,3'-azofurazane (a) and 3,3'-azobis(6-amino-1,2,4,5-tetrazine) (b) were reported in literature so far (Scheme 1).^[6]



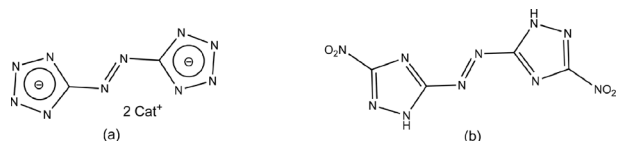
Scheme 1. Structures of some heterocyclic compounds containing the azo-functionality.

The combination of a high nitrogen content with a high heat of formation led to the development of azole-based compounds containing the azo-functionality. The recently reported 5,5'-azotetrazolate anion (Scheme 2a) is such an energetic compound with a very high nitrogen content and therefore suitable for the synthesis of energetic materials. There has been increased interest in the synthesis of energetic salts based on the 5,5'-azotetrazolate anion, since the neutral compound decomposes at room temperature.^[7] Many 5,5'-azotetrazolate salts have found practical application in combination with nitrogen-rich bases (e.g. guanidinium, triaminoguanidinium, hydrazinium) as propellants,^[8] in gas generators for airbags as well as in fire extinguishing systems.^[9] Heavy metal salts were used as initiators^[10] and derivatives of 5,5'-azotetrazole are utilized as additives in solid rocket propellants.^[11]

* Prof. Dr. T. M. Klapötke
Fax: +49-89-2180-77492

E-Mail: tmk@cup.uni-muenchen.de

[a] Energetic Materials Research, Department of Chemistry
Ludwig-Maximilian University Munich
Butenandtstr. 5–13
81377 München, Germany



Scheme 2. Structures of the 5,5'-azotetrazolate anion (a) and 3,3'-dinitro-5,5'-azo-1H-1,2,4-triazole (b).

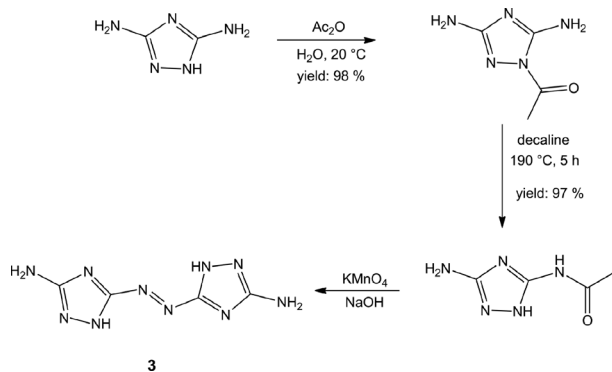
Since triazole derivatives often tend to be thermally and kinetically more stable than their tetrazole analogous, research in this field of azo-bridged azoles shows great promise for energetic materials. For example, 5,5'-dinitro-3,3'-azo-1H-1,2,4-triazole (Scheme 2b) and its nitrogen-rich salts are in the focus as potential insensitive high nitrogen compounds and propellant burn rate modifiers.^[12]

The literature known 5,5'-dinitro-3,3'-azo-1H-1,2,4-triazole was first synthesized at Los Alamos National Laboratories by Naud and co-workers in 2003.^[13] Since this molecule and selected nitrogen-rich salts like the triaminoguanidinium compound reveal a high stability and attractive explosive properties,^[14] our goal was the preparation of the corresponding nitrimino compound, as this substituent is known for its performance enhancing characteristics.

Results and Discussion

Synthesis

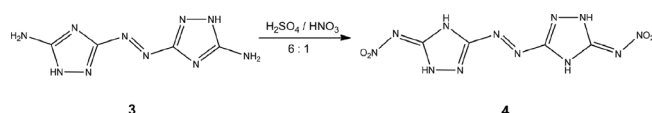
The starting material used for nitration, 5,5'-diamino-3,3'-azo-1H-1,2,4-triazole (**3**), is not yet known in literature, since it is not accessible using 3,5-diamino-1H-1,2,4-triazole as a starting material. The formation of the azo-bridge works apparently only with a unique amino group in the molecule, which necessitates the protection of one amino group first. The acetyl protecting group is suitable due to the fact that it is stable even in concentrated acids/bases at room temperature and the amine is not deprotected until using elevated temperatures. Theoretically, acylation of 3,5-diamino-1H-1,2,4-triazole can proceed both at the heterocyclic nitrogen atoms and at the two amino groups.^[15] The treatment of 3,5-diamino-1H-1,2,4-triazole with acetic anhydride in water provides 1-acetyl-diaminotria-



Scheme 3. Reaction pathway towards 5,5'-amino-3,3'-azo-1H-1,2,4-triazole starting from 3,5-diamino-1H-1,2,4-triazole.

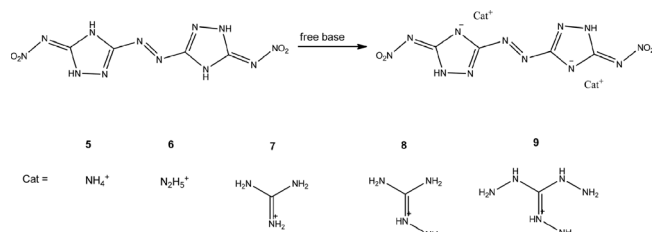
zole (**1**) in yields of about 98 %. The desired 5-acetylaminotriazole (**2**) is obtained in nearly quantitative yields with thermal isomerization by heating a suspension of **1** in decalin (Scheme 3) as it is described by Pevzner et al.^[16]

As shown in Scheme 3, the synthesis of 5,5'-diamino-3,3'-azo-1H-1,2,4-triazole (**3**) (DAAT) was performed with a stoichiometric amount of potassium permanganate, which was added at 0 °C. After removal of the ice bath, the mixture was allowed to warm to room temperature. Subsequent heating to 100 °C for 3 hours completes the formation of the azo-bridge, transforms the remaining permanganate to manganese(IV) oxide and leads to a complete deprotection of both amine groups. After the removal of the generated manganese oxide by filtration, acidifying the solution to pH 7 leads to the precipitation of compound **3** as an orange solid. Drying at 110 °C overnight provides DAAT as elemental analysis pure orange powder. The synthesis of the novel 5,5'-dinitrimino-3,3'-azo-1H-1,2,4-triazole (**4**) was accomplished in good yields via nitration of 5,5'-diamino-3,3'-azo-1H-1,2,4-triazole (**3**) as it is described for 3-amino-1H-1,2,4-triazole by Licht et al.^[17] using a volume ratio H₂SO₄/HNO₃ of 6:1 and two equivalents of nitric acid per amine group (Scheme 4).



Scheme 4. Synthesis of 5,5'-dinitrimino-3,3'-azo-1H-1,2,4-triazole (**4**) via nitration of **3**.

DNAAT immediately precipitates as a yellow solid, while pouring the nitration mixture on ice and can easily be isolated by filtration. After drying at 60 °C, the desired elemental analysis pure nitrimino compound (**4**) was obtained in yields of about 80 %. The synthesis of the nitrogen-rich salts (**5–9**) was accomplished as shown in Scheme 5 by adding two equivalents of an organic base (ammonia, hydrazine, guanidine, amidoguanidine, triaminoguanidine) to a suspension of the neutral compound in water.



Scheme 5. Synthesis of nitrogen-rich salts **5–9** of DNAAT.

The energetic salts of the dianion DNAAT^{2–} were obtained in good yields as yellow powder, while storing the mixture at 5 °C overnight. All energetic compounds were fully characterized by IR and Raman as well as multinuclear NMR spectroscopy, mass spectrometry, and differential scanning calorimetry. Selected compounds were additionally characterized by low temperature single-crystal X-ray spectroscopy.

Table 1. NMR signals of compounds **1**, **2**, **2a**, and **3a**.

Compound	¹ H NMR		¹³ C{ ¹ H} NMR		
	CH ₃	C=O	C–NH ₂	C–NHAc ^{a)}	CH ₃
1	2.33	170.5	162.2, 157.0		23.6
2	1.99	169.8	161.6	156.4	22.9
2a	2.03	174.1	162.5	154.1	22.7
3a	—	—	165.0	170.0	—

a) C–azo in the case of **3a**.

Table 2. NMR signals of compounds **4–9**.

Compound	DNAAT ^{2–} ¹ H	¹³ C{ ¹ H}	¹⁴ N{ ¹ H}	cation ¹ H	¹⁴ N{ ¹ H}
4	/	159.7, 153.8	–19	/	/
5	13.58	167.7, 158.3	–14	7.23	–359
6	13.51	166.9, 157.8	–16	7.28	–359
					¹³ C{ ¹ H}
7	13.53	167.1, 157.9	–14	7.03	157.7
8	13.61	167.0, 157.7	–15	7.89, 4.71	158.9
9	13.48	167.3, 157.8	–14	8.59, 4.49	159.0

NMR Spectroscopy

Due to the low solubility of compounds **2** and **3** in common NMR solvents (but good solubility in bases), NMR spectroscopy was performed in D₂O adding a stoichiometric amount of sodium hydroxide. The NMR signals given in Table 1 correspond to the sodium salts of **2a** and **3a** and present as well the neutral compounds **1** and **2** in [D₆]DMSO.

In the case of compound **2** (**2a**), two different NMR signals for the triazole carbon atoms could be obtained due to the rearrangement of the acetyl protecting group. The NMR signals of the two carbon atoms of compound **3a** can be found at 170.0 and 165.0 ppm in the ¹³C NMR spectra. The signals of the acetyl protecting group at 2.03 ppm (¹H NMR) and 22.7 ppm (¹³C NMR) could not be obtained anymore, indicating full deprotection of the amine groups. The signals in the NMR spectra for compounds **4–9** were recorded in [D₆]DMSO and are compiled in Table 2. The neutral compound **4** shows two signals for the different carbon atoms at δ = 159.7 and 153.8, the nitrimino group is visible at –19 ppm in the ¹⁴N NMR spectra. As expected in the case of compounds **5–9**, all NMR signals are nearly identical. The single proton localized at the triazole ring appears at chemical shifts between 13.5–13.6 ppm in the ¹H NMR spectra, whereas the signals of the two triazole carbon atoms can be found in the range between 166.9–167.7 ppm and 157.7–158.3 ppm. The nitrimino group is identified by a broad signal at around –15 ppm in the ¹⁴N NMR spectra.

Vibrational Spectroscopy

The isomerization reaction can easily be monitored by IR spectroscopy and is indicated by the shift of the C=O band from 1709 cm^{–1} (**1**) to 1683 cm^{–1} (**2**).

The complete deprotection of the amine groups during the synthesis of **3** can easily be monitored by the missing C=O vibration band at around 1700 cm^{–1} as well as the missing C–H valence vibrations at 2800–3100 cm^{–1} in the IR and Raman spectra. The latter is dominated by the absorption of the azo-moiety at 1348 cm^{–1}^[7c,18] the infrared spectrum by the deformation mode of the amino groups at 1624 cm^{–1}.

The Raman spectra of **4** are dominated by the vibration of the azo-moiety at 1436 cm^{–1}, the absorption of the amine groups in the infrared spectrum at 1624 cm^{–1} has disappeared. The N–NO₂ groups result in a strong absorption at 1620–1560 cm^{–1} [$\nu_{\text{asym}}(\text{NO}_2)$] and 1300–1240 cm^{–1} [$\nu_{\text{sym}}(\text{NO}_2)$].

The symmetric and N=O valence vibrations of all nitrogen-rich salts **5–9** can be found at 1530 cm^{–1} [$\nu_{\text{sym}}(\text{NO}_2)$] and 1335 cm^{–1} [$\nu_{\text{asym}}(\text{NO}_2)$] in the IR spectrum, accompanied by the fundamental frequencies of the triazole ring in the range of 1300–1500 cm^{–1}^[19]. The N–H stretch modes of the amine group of the cations appear in the range of 3350 cm^{–1} to 3100 cm^{–1} and the –NH₂ deformation vibration at 1630–1680 cm^{–1}. The very intense band of the azo-moiety at 1463 cm^{–1} in the Raman spectrum shows only a marginal shift in comparison to the neutral compound **4**.

Structural Characterization

The single-crystal X-ray diffraction data of **4**, **5**, and **9** were collected with an Oxford Xcalibur3 diffractometer equipped with a Spellman generator (voltage 50 kV, current 40 mA) and a Kappa CCD detector. The data collection was undertaken using the CRYSTALIS CCD software,^[20] while the data reduction was performed with the CRYSTALIS RED software.^[21] The structures were solved with SIR-92^[22] or SHELXS-97^[23] and refined with SHELXL-97^[24] implemented in the program

Table 3. Crystallographic data and parameters.

	4·DMSO	4·THF	5·DMSO	9
Formula	C ₄ H ₄ N ₁₂ O ₄ ·4 DMSO	C ₄ H ₄ N ₁₂ O ₄ ·4THF	C ₄ H ₁₀ N ₁₄ O ₄ ·2DMSO	C ₆ H ₂₄ N ₂₄ O ₆
FW /g·mol ⁻¹	596.70	572.6	474.52	528.49
Crystal system	monoclinic	monoclinic	triclinic	monoclinic
Space group	P ₂ ₁ /c	P ₂ ₁ /n	P ₁	P ₂ ₁ /c
Color / Habit	Yellow plate	Yellow rod	Yellow plate	Yellow rod
Size /mm	0.13 × 0.12 × 0.03	0.55 × 0.08 × 0.05	0.14 × 0.05 × 0.05	0.22 × 0.08 × 0.02
a /Å	17.2749(6)	5.9430(6)	7.7810(9)	9.7903(11)
b /Å	15.8671(8)	15.3647(17)	8.2010(9)	3.6340(5)
c /Å	9.7594(4)	15.2456(10)	9.0610(10)	29.233(4)
α /°	90	90	86.453(9)	90
β /°	100.068(4)	96.237(10)	81.497(9)	96.424(11)
γ /°	90	90	68.331(10)	90
V /Å ³	2633.88(19)	1383.9(3)	531.42(10)	1033.5(2)
Z	4	2	1	2
ρ _{calcd} /g·cm ⁻³	1.505	1.374	1.483	1.698
μ /mm ⁻¹	0.422	0.108	0.308	0.145
F(000)	1248	608	248	552
λ _{Mo-Kα} /Å	0.71073	0.71073	0.71073	0.71073
T /K	173	173	173	173
Theta min-max /°	4.2–28.80	4.2–26.50	4.55–26.50	4.15–26.50
Dataset <i>h</i>	−20; 22	−7; 7	−6; 9	−12; 12
Dataset <i>k</i>	−19; 18	−17; 19	−6; 10	−3; 4
Dataset <i>l</i>	−7; 13	−8; 19	−8; 11	−36; 36
Reflections collected	12529	6392	3720	4163
Independent reflections	5979	2827	2179	2129
Observed reflections	2609	1284	1122	1272
No. parameters	437	205	141	190
R _{int}	0.055	0.045	0.038	0.033
R ₁ , wR ₂ (<i>I</i> > <i>σI</i>)	0.0386; 0.0440	0.058; 0.143	0.0406; 0.0549	0.0510; 0.1275
R ₁ , wR ₂ (all data)	0.1190; 0.0509	0.132; 0.161	0.0999; 0.0611	0.0881; 0.1381
S	0.663	0.856	0.742	0.899
Resd. dens. /e·Å ⁻³	−0.375, 0.312	−0.313, 0.282	−0.241; 0.245	−0.217; 0.693
Device type	Oxford Xcalibur3 CCD	Oxford Xcalibur3 CCD	Oxford Xcalibur3 CCD	Oxford Xcalibur3 CCD
Solution	SIR-92	SHELXS-97	SHELXS-97	SHELXS-97
Refinement	SHELXL-97	SHELXL-97	SHELXL-97	SHELXL-97
Absorption correction	multi-scan	multi-scan	multi-scan	multi-scan
CCDC	807480	807481	807482	807483

package WinGX^[25] and finally checked using PLATON.^[26] Further information regarding the crystal-structure determination have been deposited with the Cambridge Crystallographic Data Centre.^[27] Crystallographic data and parameters as well as the crystal morphology are compiled in Table 3.

The crystallization of azo-bridged triazole compounds is very difficult due to the completely planar configuration of the molecules and a lack of possibilities for hydrogen bonding. We were finally able to crystallize **4** from DMSO and also THF, but were not able to record a crystal structure of the neutral compound without incorporated solvent molecules. The same problem occurred with the ionic compounds. Only the ammonium salt (**5**) and the triaminoguanidinium salt (**9**) could be crystallized after a number of tries with different solvents and crystallization conditions. Whereas **5** could only be crystallized with incorporated solvent molecules (DMSO), **9** crystallized with two molecules of crystal water per formula unit. Due to this circumstances, the structures of **4·DMSO**, **4·THF** and **5·DMSO** will not be discussed in detail since no results can be drawn from the discussion of the structure, thus only selected parameters and the asymmetric units of the compounds are

presented. The structure of the title compound **9** is discussed in detail.

The DMSO adduct of 5,5'-dinitrimino-3,3'-azo-1*H*-1,2,4-triazole (**4**) crystallizes in the monoclinic space group P₂₁/c with four molecular moieties in the unit cell, whereas the THF adduct crystallizes in the monoclinic space group P₂₁/n with only two molecular moieties in the unit cell. Pycnometer measurements of **4** stated a density of 1.85 g·cm⁻³, whereas the densities derived from the crystallographic measurements are very low with 1.505 g·cm⁻³ for **4·DMSO** and 1.374 g·cm⁻³ for **4·THF**, respectively, owed to the solvent incorporation. The asymmetric units for both adducts are displayed in Figure 1 and Figure 2 together with the numbering scheme and selected bond lengths and angles.

The DNAAT molecule is nearly planar in both structures, indicating the presence of a delocalized π-electron system, as anticipated for these compounds. Bond lengths and angles are also as expected for this kind of compounds.^[28] The bond length of the azo moiety is in the same range as for the azotetrazole compounds investigated by Hammerl,^[7c, 29] while the nitraminogroups also exhibit regular geometrical parameters.

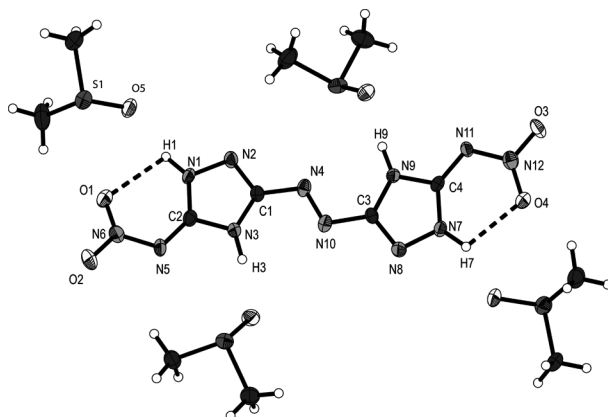


Figure 1. Molecular moiety of **4·DMSO**. Thermal ellipsoids represent the 50 % probability level. Selected bond lengths /Å: O1–N6 1.243(3), O2–N6 1.242(3), N1–C2 1.340(3), N1–N2 1.370(3), N1–H1 0.90(2), N2–C1 1.307(3), N3–C2 1.352(3), N3–C1 1.355(3), N3–H3 0.913(16), N4–N10 1.280(3), N4–C1 1.397(3), N5–C2 1.341(3), N5–N6 1.343(3); selected bond angles /°: C2–N1–N2 111.9(2), C2–N1–H1 132.8(16), N2–N1–H1 115.2(16), C1–N2–N1 103.1(2), C2–N3–C1 106.3(2), C2–N3–H3 119.7(15), C1–N3–H3 133.8(16), N10–N4–C1 111.8(2), C2–N5–N6 115.7(2), O2–N6–O1 122.0(2), O2–N6–N5 115.7(3), O1–N6–N5 122.3(3), C4–N7–N8 112.46(19), C4–N7–H7 128.8(15), N2–C1–N3 112.9(2), N2–C1–N4 119.3(3), N3–C1–N4 127.4(2), N1–C2–N5 135.9(2), N1–C2–N3 105.8(2), N5–C2–N3 118.2(3).

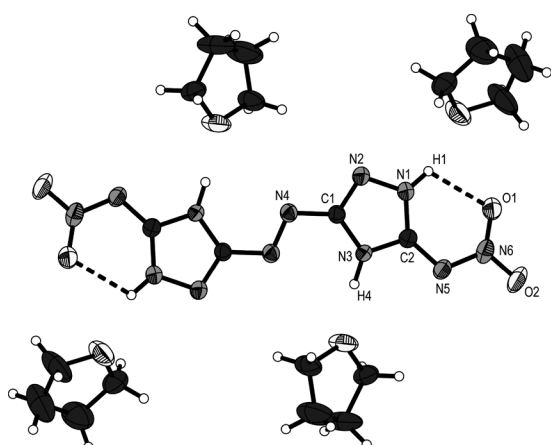


Figure 2. Molecular moiety of **4·THF**. Thermal ellipsoids represent the 50 % probability level. Selected bond lengths /Å: C4–C3 1.406(5), C4–C5 1.424(6), N6–1.244(3), N1–C2 1.356(4), N1–N2 1.368(3), N1–H1 0.88(3), N2–C1 1.308(3), N5–C2 1.339(4), N5–N6 1.356(3), N4–N4 1.272(4), N4–C1 1.392(3), N3–C2 1.346(3), N3–C1 1.368(4), N3–H4 0.94(3), N6–O2 1.239(3); selected bond angles /°: C2–N1–N2 111.8(3), C2–N1–H1 129(2), N2–N1–H1 119(2), C1–N2–N1 103.6(2), C2–N5–N6 115.6(3), N4–N4–C1 112.2(3), C2–N3–C1 106.8(2), C2–N3–H4 125(2), C1–N3–H4 128(2), O2–N6–O1 121.5(3), O2–N6–N5 116.0(3), O1–N6–N5 122.4(2), N5–C2–N3 119.8(3), N5–C2–N1 134.8(3), N3–C2–N1 105.5(3), N2–C1–N3 112.3(2), N2–C1–N4 120.8(2), N3–C1–N4 127.0(2).

The interesting aspect of both structures is the presence of moderately strong intramolecular hydrogen bonds. N1 and N7 are utilized as donor atoms with O1 and O4 function as acceptor atoms respectively for **4·DMSO**, while N1 and O1 build

up the hydrogen bond for **4·THF**. Even though, the D–H···A angles are pretty small with 102.15(16)° (N1–H1···O1, **4·DMSO**), 105.8(1)° (N7–H7···O4, **4·DMSO**) and 108.21(23)° (N1–H1···O1, **4·THF**), the D–A distances are very small, ranging between 2.587(1) Å (N1–O1, **4·THF**) and 2.606(4) Å (N1–O1, **4·DMSO**). The hydrogen bonds are considered to be of electrostatic nature rather than being directed.^[30] The build-up of a six-membered ring between the nitrimino group and the triazole ring, is making the backbone of the molecule more stable, which is also indicated by the very high thermal stabilities, unusual for this class of compounds. In addition the hydrogen atom can only be deprotonated with the use of earth alkaline bases, not with the bases used to form the di-anion. Further, the incorporated solvent molecules take their space due to the formation of hydrogen bonds with each of the four N–H hydrogen atoms. Thus both structures show the mutual number of solvent molecules surrounding each DNAAT molecule.

Bis(ammonium) 5,5'-dinitrimino-3,3'-azo-1*H*-1,2,4-triazolate (**5·DMSO**) crystallizes in the triclinic space group $P\bar{1}$, formally with only one molecular moiety occupying the unit cell. The density is as expected very low with only 1.483 g·cm⁻³ due to the formation of the DMSO adduct. One molecular moiety together with selected bond length and angles is presented in Figure 3.

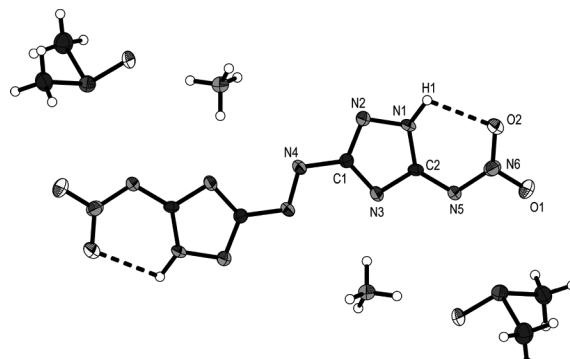


Figure 3. Molecular moiety of **5**. Thermal ellipsoids represent the 50 % probability level. Selected bond lengths /Å: O1–N6 1.270(2), O2–N6 1.260(2), N1–C2 1.345(3), N1–N2 1.368(2), N1–H1 0.917(15), N2–C1 1.327(3), N3–C2 1.335(3), N3–C1 1.356(3), N4–N4 1.278(3), N4–C1 1.413(3), N5–N6 1.322(2), N5–C2 1.381(3); selected bond angles /°: C2–N1–N2 110.46(19), C2–N1–H1 133.0(14), N2–N1–H1 116.5(14), C1–N2–N1 101.00(19), C2–N3–C1 102.0(2), N4–N4–C1 112.0(2), N6–N5–C2 116.8(2), O2–N6–O1 120.4(2), O2–N6–N5 123.6(2), O1–N6–N5 116.1(2), N2–C1–N3 116.5(2), N2–C1–N4 117.4(2), N3–C1–N4 126.2(2), N3–C2–N1 110.1(2), N3–C2–N5 117.9(2), N1–C2–N5 132.0(2).

The dianion is completely planar within the ionic structures with only very slight deviations. The N1–H1···O2 hydrogen bond builds up the six membered ring again, as seen for the neutral compound, keeping the nitrimino group perfectly in plane with the triazole ring. Since the thermal decomposition temperature differs only by 3 °C when compared with **4** [209 °C (**4**) compared to 212 °C (**5**)] the formation of this stable configuration seems to have a very important impact on the stability of these compounds. The structure itself is build

Table 4. Hydrogen bonds present in the crystal structure of **5**. Since the N–H bonds of the ammonium ion had to be set as restraint, no standard deviation is presented.

Atoms D–H–A	Dist D–H /Å	Dist. H–A /Å	Dist. D–A /Å	Angle D–H–A /°
N1–H1–O3 ⁱ	0.917(15)	1.937(18)	2.786(3)	153.0(19)
N7–H7a–O1 ⁱⁱ	0.96	2.00	2.929(2)	163.8
N7–H7b–O3	0.92	1.91	2.811(2)	167.1
N7–H7c–N3	0.92	1.98	2.872(3)	164.3

Symmetry operators: (i) $x, y-1, z$; (ii) $x+1, y, z$; (iii) $-x+1, -y+1, -z$.

Table 5. Hydrogen bonds present in the crystal structure of **9**. H7, H8 and H9 had to be set restraint, thus no standard deviations are given for the D–H and H–A distances as well as for the D–H–A angles.

Atoms D–H–A	Dist. D–H /Å	Dist. H–A /Å	Dist. D–A /Å	Angle D–H–A /°
N1–H1–O1	0.770(4)	2.256(37)	2.579(9)	106.2(9)
N1–H1–O3	0.77(3)	1.98(4)	2.733(3)	165(4)
N7–H7–O1 ⁱ	0.88	2.34	2.995(3)	130.9
N8–H8–O2 ⁱⁱ	0.88	2.18	2.954(3)	146.3
N9–H9–N5 ⁱⁱⁱ	0.88	2.37	3.186(3)	153.7
N10–H10a–O1	0.96(4)	2.14(4)	3.075(4)	163(3)
N10–H10b–N10 ⁱⁱ	0.83(4)	2.52(4)	3.198(4)	140(3)
N10–H10b–O2 ⁱ	0.83(4)	2.57(4)	3.126(3)	125(3)
N11–H11a–N11 ^{iv}	0.827(19)	2.63(3)	3.142(5)	121(3)
N11–H11a–O2 ⁱⁱⁱ	0.827(19)	2.54(3)	3.147(3)	131(3)
N11–H11b–N5 ^v	0.82(4)	2.37(4)	3.176(4)	168(3)
N12–H12a–N4 ^{vi}	0.82(4)	2.46(4)	3.189(3)	148(3)
N12–H12b–N3 ⁱⁱⁱ	0.87(4)	2.20(4)	3.000(3)	154(3)
N12–H12a–O3	0.82(4)	2.71(3)	3.197(9)	119.6(3)
O3–H3a–N12 ^{vii}	0.73(4)	2.31(4)	3.000(3)	159(4)
O3–H3b–N2 ^{vi}	0.91(4)	2.04(4)	2.922(3)	163(4)

Symmetry operators: (i) $x, y+1, z$; (ii) $-x+1, y+1/2, -z+1/2$; (iii) $x-1, y+1, z$; (iv) $-x, y+1/2, -z+1/2$; (v) $x-1, y, z$; (vi) $-x+1, -y+1, -z$; (vii) $x, y-1, z$.

up from four moderately stable hydrogen bonds, all four of them involving the ammonium cation. An illustration of the surrounding of one ammonium cation is presented in Figure 4, whereas the parameters of the hydrogen bonds are compiled in Table 4.

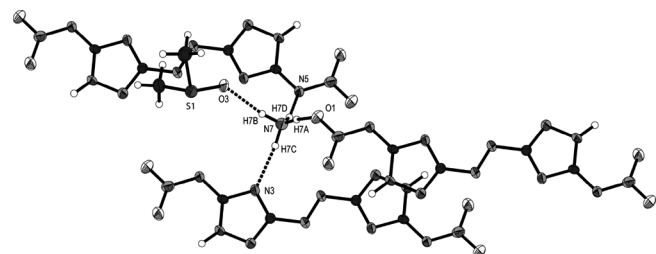


Figure 4. Chemical surrounding of the ammonium cation in **5**, displaying the hydrogen bonds. Thermal ellipsoids represent the 50 % probability level.

The dihydrate of the bis(triaminoguanidinium) 5,5'-dinitrimino-3,3'-azo-1*H*-1,2,4-triazolate (**9**) crystallizes in the monoclinic space group *P*2₁/*c* with two formula units in the unit cell. The density is in the same range as other guanidinium salts of nitrimino compounds with 1.698 g·cm⁻³. The density is also in good agreement with the experimentally determined density of the anhydrous compound being 1.72 g·cm⁻³ (pyc-

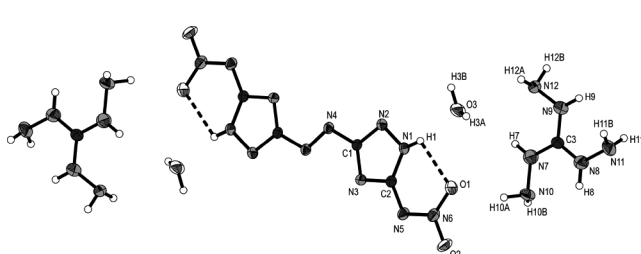
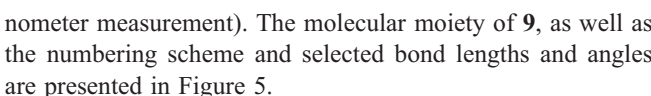


Figure 5. Molecular moiety of **9**. Thermal ellipsoids represent the 50 % probability level. Selected bond lengths /Å: O1–N6 1.264(3), O2–N6 1.255(3), N1–N2 1.351(3), N1–C2 1.354(3), N1–H1 0.77(3), N2–C1 1.323(3), N3–C2 1.336(3), N3–C1 1.344(3), N4–N4 1.277(4), N4–C1 1.407(3), N5–N6 1.310(3), N5–C2 1.368(3), N7–C3 1.313(3), N7–N10 1.431(3), N8–C3 1.316(4), N8–N11 1.406(3), N9–C3 1.331(4), N9–N12 1.419(3); selected bond angles /°: N2–N1–C2 110.2(2), N2–N1–H1 116(3), C2–N1–H1 134(3), C1–N2–N1 101.8(2), C2–N3–C1 102.5(2), N4–N4–C1 111.9(3), N6–N5–C2 117.7(2), O2–N6–O1 120.8(2), O2–N6–N5 116.9(2), O1–N6–N5 122.2(2), N2–C1–N3 116.2(2), N2–C1–N4 116.7(2), N3–C1–N4 127.1(2), N3–C2–N1 109.4(2), N3–C2–N5 118.2(2), N1–C2–N5 132.4(2), C3–N7–N10 118.3(2), C3–N8–N11 121.9(3), C3–N9–N12 119.0(2).

As seen in the structure of **5**, the DNAAT²⁻ anion is completely planar. The structural motive of two six-membered rings, stabilizing the nitrimino groups is also evident in this structure. The donor acceptor distance is in the same range as for **4** and **5** with 2.579(9) Å and with the D-H...A angle of 106.22(31)° of strong electrostatic nature. The complete structure is build up by a strong hydrogen network including 15 non-equivalent hydrogen bonds. All hydrogen bonds are compiled in Table 5.

The structure consists of coplanar bands, build up from DNAAT²⁻ anions, water molecules and triaminoguanidinium cations located approximately 1 Å below and above the layer spanned up by DNAAT²⁻ anions. The water molecules are located between the DNAAT²⁻ molecules forming strong and directed hydrogen bonds with the triazole rings, namely N1-H1...O3 and O3-H3b...N2^{vi}. These hydrogen bonds are well below the sum of van der Waals radii [$r_w(N) + r_w(O) = 3.10$ Å].^[31] The third hydrogen bond is formed by the water molecule as donor, whereas N12^{vii} functions as the donor. Again, the D-A distance is much shorter than the sum of van der Waals radii and the D-H...A angle is 159°, which again indicates a rather directed than only electrostatic interaction. The only weak hydrogen bond build up by the H₂O is N12-H12a...O3, with a donor acceptor distance of 3.197(9) Å and therefore longer than the sum of van der Waals radii and an D-H...A angle of only 119.6(3)°. All other hydrogen bonds formed are using the nitrogen atoms of the triaminoguanidinium cation as donor atoms. The two hydrogen bonds utilizing nitrogen atoms of the DNAAT²⁻ anion as acceptors all show D-A distances smaller than the sum of van der Waals radii [$r_w(N) + r_w(N) = 3.2$ Å] at 3.186 Å (N9-H9-N5ⁱⁱⁱ) and 3.000 Å (O3-H3a-N12^{vii}), respectively. The corresponding D-H...A angles (around 150°) indicate the bonds being moderately strong but mostly of electrostatic nature. The three hydrogen bonds using oxygen atoms as acceptors are moderately strong with D-A distances between 2.954 and 3.147 Å and with D-H...A angles between 125° and 131° they are rather of electrostatic nature. The complete hydrogen bonding scheme within the bands is presented in Figure 6.

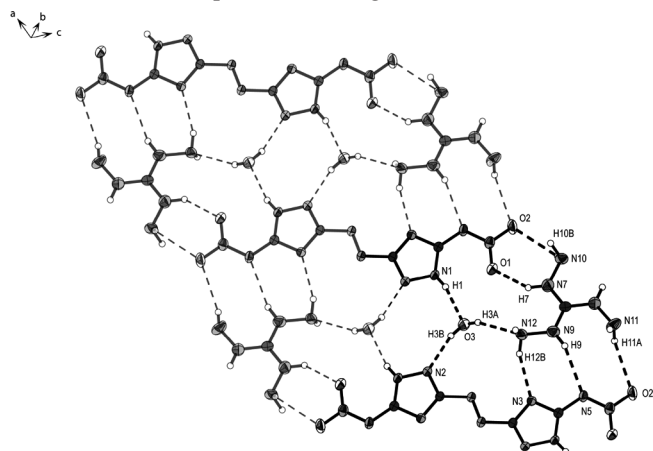


Figure 6. Hydrogen bonding scheme within the band structures of **9**. Thermal ellipsoids represent the 50 % probability level.

The distance between the bands is 3.280 Å, whereas they are stacked along the *b* axis. The bands are connected by hydrogen

bonds formed between the triaminoguanidinium cations and interactions from the triaminoguanidinium cation with the nitramino groups, to form zigzag layers presenting an angle of 133.99° between the individual bands. The hydrogen bonds involved are namely N11-H11a...N11^{iv} and N10-H10b...N10ⁱⁱ, only involving the triaminoguanidinium cations, whereas N8-H8...O2ⁱⁱ presents the interaction between the NH group of the triaminoguanidinium cation in one layer with the nitrimino group of the DNAAT²⁻ anion in the tilted layer. The layer scheme of the structure is displayed in Figure 7 along the *a* axis.

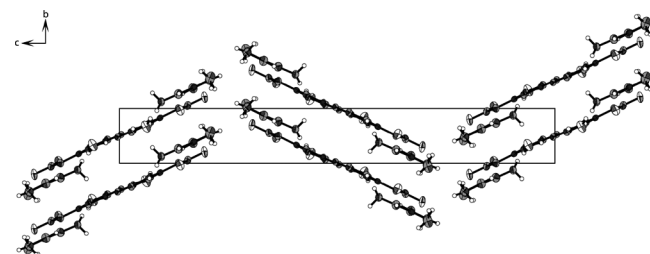


Figure 7. Layer structure of **9**, showing the connectivity of the individual bands along the *a* axis. Thermal ellipsoids represent the 50 % probability level.

The angle between the bands is due to the connectivity over hydrogen bonds formed by the triaminoguanidinium cations. The N10-H10b...N10ⁱⁱ and N11-H11a...N11^{iv} hydrogen bonds are rather long with D-A distances of 3.142 and 3.198 Å, respectively, but shorter than the sum of van der Waals radii. D-H...A angles of only 121° and 140°, respectively, indicate mostly electrostatic interactions. Since the donor atoms are the two amine groups, the angle between the bands is given. The third band connecting hydrogen bond N8-H8...O2ⁱⁱ is rather short with a D-A distance of 2.954 Å. The bond is mainly of electrostatic nature, but also directed with a D-H...A angle of

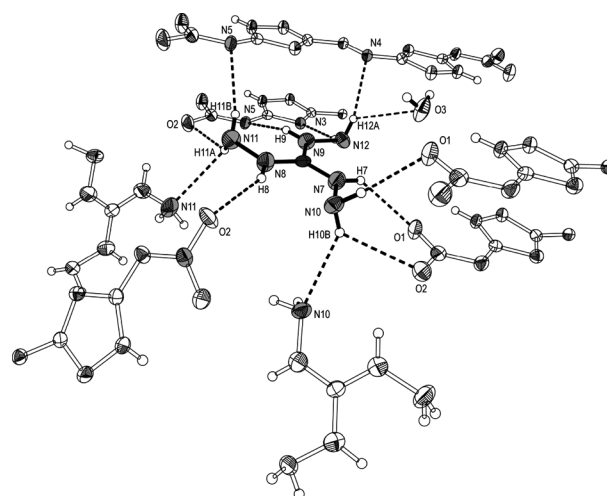


Figure 8. Surrounding of one triaminoguanidinium cation in **9**, showing the connectivity of the structural motive. Non participating atoms are set transparent, molecules are partially omitted for better clarity. Thermal ellipsoids represent the 50 % probability level.

146.43°. The surrounding of one triaminoguanidinium cation is displayed in Figure 8, presenting the complete three dimensional hydrogen bonding network. Three moderately strong hydrogen bonds connect the bands towards the next layer, namely N11–H11b…N5^v, N12–H12a…N4^{vi}, and N10–H10a…O1.

Theoretical Calculations

Due to the highly energetic character of **4–9**, bomb calorimetric measurements could only be performed with small amounts; consequently doubtful combustion energies were obtained. Therefore an extensive computational study was accomplished for **4–9**, which is presented in the following section. All calculations were carried out using the Gaussian G03W (revision B.03) program package.^[32] The enthalpies (H) and free energies (G) were calculated using the complete basis set (CBS) method of Petersson and co-workers in order to obtain very accurate energies. The CBS models use the known asymptotic convergence of pair natural orbital expressions to extrapolate from calculations using a finite basis set to the estimated complete basis set limit. CBS-4 begins with a HF/3-21G(d) geometry optimization; the zero point energy is computed at the same level. Subsequently, it uses a large basis set SCF calculation as a base energy, and a MP2/6-31+G calculation with a CBS extrapolation to correct the energy through second order. A MP4(SDQ)/6-31+(d,p) calculation is used to approximate higher order contributions. In this study we applied the modified CBS-4M method (M referring to the use of Minimal Population localization), which is a re-parameterized version of the original CBS-4 method and also includes some additional empirical corrections.^[33] The enthalpies of the gas-phase species M were computed according to the atomization energy method [Equation (1)] (Table 6, Table 7, and Table 8).^[34]

$$\Delta_f H^\circ_{(g,M,298)} = H_{(\text{Molecule},298)} - \sum H^\circ_{(\text{Atoms},298)} + \sum \Delta_f H^\circ_{(\text{Atoms},298)} \quad (1)$$

Table 6. Results obtained from theoretical calculations at the CBS-4M level of theory.

	point group	$-H^{298}$ /a.u.	NIMAG
DNAAT	C_1	1111.064789	0
DNAAT ²⁻	C_s	1110.009835	0
A ⁺	T_d	56.796608	0
Hy ⁺	C_s	112.030523	0
G ⁺	C_1	205.453192	0
AG ⁺	C_1	260.701802	0
TAG ⁺	C_3	371.197775	0
H		0.500991	0
C		37.786156	0
N		54.522462	0
O		74.991202	0
Cl		459.674576	0

Table 7. Literature values for atomic ΔH_f^{298} /kcal·mol⁻¹.

	NIST ^[35]
H	52.1
C	171.3
N	113.0
O	59.6
Cl	29.0

Table 8. Enthalpies of the gas-phase species M.

M	M	$\Delta_f H^\circ(g, M)$ /kcal·mol ⁻¹
DNAAT	$C_4H_4N_{12}O_4$	743.6
DNAAT ²⁻	$C_4H_2N_{12}O_4^{2-}$	446.5
A	NH_4^+	151.9
Hy	$N_2H_5^+$	184.9
G	$CH_6N_3^+$	136.6
AG	$CH_7N_4^+$	160.4
DAG	$CH_8N_5^+$	184.5
TAG	$CH_7N_4^+$	208.8

The solid state energy of formation of DNAAT was calculated by subtracting the gas-phase enthalpy with the heat of sublimation (22.5 kcal·mol⁻¹) obtained by Trouton's rule ($\Delta H_{\text{sub}} = 188 T_m$) ($T_m = 204$ °C).^[36] In the case of the salts, the lattice energy (U_L) and lattice enthalpy (ΔH_L) were calculated from the corresponding molecular volumes (Table 9 and Table 10) according to the equations provided by Jenkins et al.^[37] With the calculated lattice enthalpy (Table 9) the gas-phase enthalpy of formation (Table 8) was converted into the solid state (standard conditions) enthalpy of formation. These molar standard enthalpies of formation (ΔH_m) were used to calculate the molar solid state energies of formation (ΔU_m) according to Equation (2) (Table 7).

$$\Delta U_m = \Delta H_m - \Delta n RT \quad (2)$$

(Δn being the change of moles of gaseous components)

Detonation Parameters and Thermal Properties

The calculation of the detonation parameters was performed with the program package EXPLO5 (version 5.03 and 5.04).^[38] The program is based on the chemical equilibrium, steady-state model of detonation. It uses the Becker–Kistiakowsky–Wilson equation of state (BKW EOS) for gaseous detonation products and the Cowan–Fickett equation of state for solid carbon. The calculation of the equilibrium composition of the detonation products is done by applying a modified White–Johnson–Dantzig free energy minimization technique. The program is designed to enable the calculation of detonation parameters at the CJ point. The BKW equation in the following form was used with the BKWN set of parameters ($\alpha, \beta, \kappa, \theta$) as stated below the equations and X_i being the mol fraction of i -th gaseous product, k_i is the molar co-volume of the i -th gaseous product:^[39]

$$pV / RT = 1 + xe^{\beta x} x = (\kappa \sum X_i k_i) / [V(T + \theta)]^\alpha$$

$$\alpha = 0.5, \beta = 0.176, \kappa = 14.71, \theta = 6620.$$

The detonation parameters calculated with the EXPLO5 versions V5.03 and V5.04 using the experimentally determined densities (X-ray) are summarized in Table 11.

The neutral compound **4** already shows a remarkably high thermal stability of 209 °C, but a quite high sensitivity towards friction and impact. Since salts of energetic compound tend to be more stable as the neutral compound, the nitrogen-rich salts

Table 9. Lattice energies and lattice enthalpies.

	V_M /nm ³	U_L /kJ·mol ⁻¹	ΔH_L /kJ·mol ⁻¹	ΔH_L /kcal·mol ⁻¹
(NH ₄) ₂ DNAAT (5)	298	1306.1	1317.0	314.5
(N ₂ H ₅) ₂ DNAAT (6)	312	1283.5	1294.4	309.2
(G) ₂ DNAAT (7)	388	1181.0	1191.9	284.7
(AG) ₂ DNAAT (8)	464	1102.3	1113.2	265.9
(TAG) ₂ DNAAT (9)	472	1095.0	1105.9	264.1

Table 10. Solid state energies of formation ($\Delta_f U^\circ$).

	$\Delta_f H^\circ(s)$ /kcal·mol ⁻¹	$\Delta_f H^\circ(s)$ /kJ·mol ⁻¹	Δn	$\Delta_f U^\circ(s)$ /kJ·mol ⁻¹	M /g·mol ⁻¹	$\Delta_f U^\circ(s)$ /kJ·kg ⁻¹
DNAAT (4)	154.7	647.7	10	672.5	248.2	2366.3
(NH ₄) ₂ DNAAT (5)	95.8	401.2	14	435.9	318.3	1369.6
(N ₂ H ₅) ₂ DNAAT (6)	167.3	700.4	16	740.1	348.32	2124.6
(G) ₂ DNAAT (7)	95.2	398.4	18	443.0	402.4	1101.0
(AG) ₂ DNAAT (8)	161.6	676.5	20	726.1	432.42	1679.2
(TAG) ₂ DNAAT (9)	260.1	1089.2	24	1148.7	492.50	2332.3

Table 11. Physico-chemical properties of **4–9** in comparison with hexogen (RDX).

	DNAAT (4)	(NH ₄) ₂ DNAAT (5)	(N ₂ H ₅) ₂ DNAAT (6)	(G) ₂ DNAAT (7)	(AG) ₂ DNAAT (8)	(TAG) ₂ DNAAT (9)	RDX*
Formula	C ₄ H ₄ N ₁₂ O ₄	C ₄ H ₁₀ N ₁₄ O ₄	C ₄ H ₁₂ N ₁₆ O ₄	C ₆ H ₁₄ N ₁₈ O ₄	C ₆ H ₁₆ N ₂₀ O ₄	C ₆ H ₂₀ N ₂₄ O ₄	C ₃ H ₆ N ₆ O ₇
Molecular mass /g·mol ⁻¹	284.16	318.21	348.12	402.14	432.17	492.38	222.12
Impact sensitivity /J ^{a)}	2	> 40	10	> 40	> 40	> 40	7
Friction sensitivity /N ^{b)}	20	> 360	> 360	> 360	> 360	160	120
ESD-test /J	0.1	0.15	0.05	0.35	0.2	0.2	—
N /% ^{c)}	59.15	61.62	64.35	62.67	64.80	68.27	37.8
Ω /% ^{d)}	-33.78	-45.25	-45.94	-59.65	-59.21	-58.48	-21.6
T_{dec} /°C ^{e)}	209	212, 257	154, 228	261	177	219	204 (mp)
ρ /g·cm ⁻³ ^{f)}	1.85	1.70	1.70	1.70	1.70	1.70	1.80
$\Delta_f H_m^\circ$ /kJ·mol ⁻¹ ^{g)}	647.7	401.2	700.4	398.4	676.5	1089.2	70
$\Delta_f U^\circ$ /kJ·kg ⁻¹ ^{h)}	2366.3	1369.6	2124.6	1101.0	1679.2	2332.3	417
EXPLO5 values: V5.03 (V5.04)							
- $\Delta_E U^\circ$ /kJ·kg ⁻¹ ⁱ⁾	5268 (5339)	4473 (4461)	5055 (5026)	3731 (3690)	4202 (4147)	4681 (4602)	6038 (6125)
T_E /K ^{j)}	4237 (4089)	3362 (3234)	3583 (3475)	2855 (2732)	3048 (2944)	3213 (3087)	4368 (4236)
p_{C-J} /kbar ^{k)}	337 (298)	259 (267)	290 (294)	242 (241)	267 (262)	300 (290)	341 (349)
V_{Det} /m s ⁻¹ ^{l)}	8784 (8723)	8156 (8229)	8609 (8575)	8034 (7944)	8391 (8244)	8890 (8596)	8906 (8748)
Gas vol. /L·kg ⁻¹ ^{m)}	732 (708)	809 (798)	832 (816)	801 (781)	820 (797)	852 (822)	793 (739)

a) BAM dropammer, grain size (75–150 µm). b) BAM friction tester, grain size (75–150 µm). c) Nitrogen content. d) Oxygen balance.^[40] e) Temperature of decomposition by DSC ($\beta = 5$ °C, Onset values). f) Estimated density based on X-ray data from **7** and **9**, Pycnometer for DNAAT. g) Molar enthalpy of formation. h) Energy of formation. i) Energy of Explosion. j) Explosion temperature. k) Detonation pressure. l) Detonation velocity. m) Assuming only gaseous products; * values based on reference^[41] and the EXPLO5 database; n.d.: not determined.

of DNAAT are expected to show an improved stability. The decomposition temperatures of the compounds **5–9** are in the range of the neutral compound, those of the ammonium and guanidinium as well as the triaminoguanidinium salt are even higher and appear in the range from 212 °C up to 261 °C. The ammonium and the hydrazinium salts show two decomposition points in the DSC with the first decomposition starting at 212 °C and 154 °C, respectively. As expected, the sensitivity values of all nitrogen-rich salts are considerably lower in comparison to the neutral compound. Nearly all compounds are insensitive towards friction, impact and electrostatic discharge, only the hydrazinium salt is slightly sensitive towards impact (10 J) and the triaminoguanidinium salt towards friction (160 N).

The nitrogen-rich salts of DNAAT exhibit positive heats and energies of formation. The detonation velocities were calculated in the range of 7944 m·s⁻¹ (**7**) to 8596 m·s⁻¹ (**9**). The best performance was calculated for the triaminoguanidinium salt (**9**) with a detonation velocity of 8596 m·s⁻¹, which is only slightly lower than the performance of RDX. With the excellent sensitivity values for friction (160 N), impact (<40 J), and ESD (0.2 J) in addition to the remarkable high temperature of decomposition (219 °C) and a very low solubility in water (2.5 g·L⁻¹, 25 °C), the triaminoguanidinium salt (**9**) seems to be the best choice in terms of performance and sensitivity and makes this compound suitable as a potential new high explosive. Additionally, the DSC curves of the 5,5'-dinitrimino-3,3'-

azo-1*H*-1,2,4-triazole (**4**) and the corresponding bis(triaminoguanidinium) salt (**9**) are displayed in Figure 9.

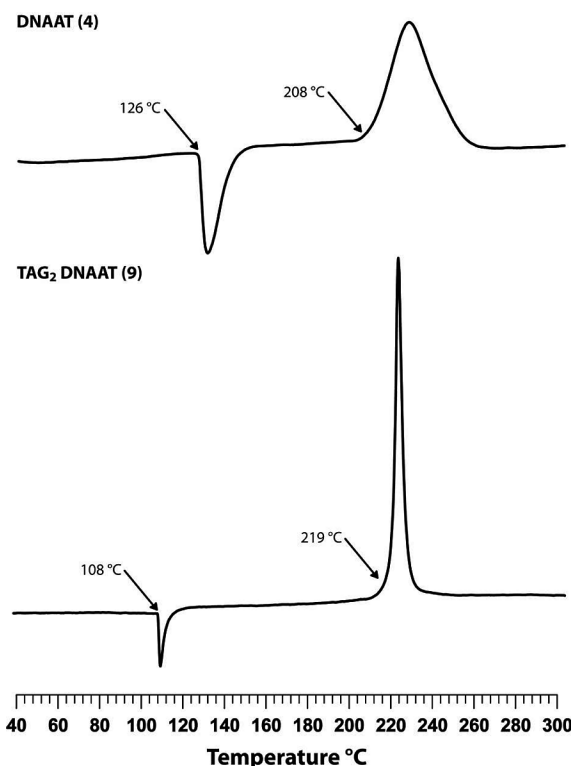


Figure 9. Differential scanning calorimetry (DSC) curves for the neutral nitrimino compound **4** and the bis(triaminoguanidinium) salt of **4** (**9**).

Since 3,5-diamino-1*H*-1,2,4-triazole was used previously as a starting material resulting in 3,3'-dinitro-5,5'-azo-1,2,4-triazole (DNAT) and its triaminoguanidinium salt,^[13, 14] we want to put the results obtained for these compounds in relation to the advances we were able to make. DNAT, synthesized by Naud et al., as mentioned in the introduction, shows a much lower sensitivity towards impact and friction with 12.5 J and 250 N, respectively, than the neutral nitrimino compound DNAAT (**4**), while the density is in the same region as observed for **4** (1.85 g·cm⁻³). DNAT as a neutral compound is therefore much more stable regarding outer stimuli, but shows lower performance characteristics than DNAAT with a detonation velocity of 8500 m·s⁻¹ (**4**: 8723 m·s⁻¹). Hence we were able to increase the performance of the molecule with the exchange of the nitro group with the nitrimino group, but the sensitivity values are much too high which prohibits the use as an energetic material (other than for primary explosives). This relation changes, when comparing the triaminoguanidinium salts of DNAT and DNAAT. In this case TAG₂ DNAAT (**9**) is exceeding the properties of TAG₂ DNAT in every respect: the decomposition temperature of **9** is higher (219 °C compared to 202 °C) together with the sensitivity values being much better in respect to the impact sensitivity (DNAT: 9.3 J, **9**: > 40 J) and close to equal with respect to the friction sensitivity (DNAT: 157 N, **9**: 160 N). The performance characteristics of **9** cannot be compared directly, since they were calculated at

different densities, but we can state an overall increase in performance. At a density of 1.58 g·cm⁻³ TAG₂ DNAT shows a detonation velocity of 8200 m·s⁻¹ and a detonation pressure at the Chapman–Jouguet point of 230 kbar, whereas **9** exhibits a detonation pressure of 8596 m·s⁻¹ paired with a detonation pressure of 290 kbar at a density of 1.70 g·cm⁻³.

Conclusions

From this combined experimental and theoretical study the following conclusions have been drawn:

The application of the very straightforward and efficient acetyl protection of 3,5-diamino-1*H*-1,2,4-triazole allows selective reactions of the remaining free amine group and establishes a basis to a multitude of potential new energetic compounds that are now accessible. The synthesis of 5,5'-diamino-3,3'-azo-1*H*-1,2,4-triazole (**3**) by reaction of 5-acetylamino-3-amino-1*H*-1,2,4-triazole (**2**) with potassium permanganate is described. Compound **3** acts as starting material for other new high energetic materials, since several modifications of the amine groups are possible. The subsequent nitration of **3** leads to the formation of 5,5'-dinitrimino-3,3'-azo-1*H*-1,2,4-triazole (**4**), which was fully characterized in terms of sensitivity and energetic properties as well as by single-crystal X-ray diffraction. The molecule reveals promising energetic properties but quite high sensitivities towards friction (20 N), impact (2 J), and electrostatic discharge (0.1 J). Therefore, nitrogen rich salts were synthesized by reaction with high-nitrogen bases (ammonia, hydrazine, guanidine, aminoguanidine, and triaminoguanidine). All salts were fully characterized by NMR-, IR-, and Raman spectroscopy. Special attention was turned on the thermal stabilities and sensitivities values. The triaminoguanidinium salt (**9**) exhibits a remarkable high temperature of decomposition (219 °C) and detonation velocity (8596 m·s⁻¹) and therefore turned out to be the most promising compound in terms of performance and stability. The performance characteristics of **9** exceed the ones of TAG₂ DNAT, which served us as a starting point regarding performance and stability, especially when comparing the detonation pressure and sensitivity values.

Experimental Section

Caution: Although all 3,5-diamino-1,2,4-triazole derivatives reported in this publication are rather stable against friction, impact, and electric discharge, proper safety precautions should be taken when handling these compounds. The derivatives are energetic materials and tend to explode under certain conditions, especially under physical stress. Laboratories and personnel should be properly grounded, and safety equipment such as Kevlar gloves, leather coats, face shields, and ear plugs are recommended.

General: All chemical reagents, except 3,5-diamino-1,2,4-1*H*-triazole and solvents were obtained from Sigma–Aldrich Inc. or Acros Organics (analytical grade) and were used as supplied. 3,5-Diamino-1,2,4-1*H*-triazole was obtained from ABCR. ¹H, ¹³C{¹H}, and ¹⁴N NMR spectra were recorded with a JEOL Eclipse 400 instrument in [D₆]DMSO at or near 25 °C. The chemical shifts are given relative to tetramethylsilane (¹H, ¹³C) or nitromethane (¹⁴N) as external standards

and coupling constants are given in Hertz (Hz). Infrared (IR) spectra were recorded with a Perkin–Elmer Spectrum BX FT-IR instrument equipped with an ATR unit at 25 °C. Transmittance values are qualitatively described as “very strong” (vs), “strong” (s), “medium” (m) and “weak” (w). Raman spectra were recorded with a Bruker RAM II spectrometer equipped with a Nd:YAG laser (1064 nm) and a reflection angle of 180°. The intensities were reported as percentages of the most intense peak and are given in parentheses. Elemental analyses were performed with a Netzsch Simultaneous Thermal Analyzer STA 429. Melting points were determined by differential scanning calorimetry (Setaram DSC141 instrument, calibrated with standard pure indium and zinc). Measurements were performed at a heating rate of 5 °C·min⁻¹ in closed aluminum sample pans with a 1 μm hole in the top for gas release in a nitrogen flow of 20 mL·min⁻¹ with an empty identical aluminum sample pan as a reference.

For initial safety testing, the impact and friction sensitivities as well as the electrostatic sensitivities were determined. The impact sensitivity tests were carried out according to STANAG 4489,^[42] modified according to instruction^[43] using a BAM^[44] dropammer. The friction sensitivity tests were carried out according to STANAG 4487^[45] and modified according to instruction^[46] using the BAM friction tester. The electrostatic sensitivity tests were accomplished according to STANAG 4490^[47] using an electric spark testing device ESD 2010EN (OZM Research) operating with the “Winspark 1.15 software package”.

1-Acetyl-3,5-diamino-1*H*-1,2,4-triazole (1): According to literature,^[16] acetic anhydride (40.8 mL, 1.2 equiv.) was added dropwise under vigorous stirring to a solution of 3,5-diamino-1,2,4-triazole (36.0 g, 0.36 mol) in 130 mL water at room temperature. After stirring for 1 h, the precipitate was filtered off, washed with water, and dried at room temperature to yield **1** as a colorless powder (48.3 g, 0.34 mol, 95 % 1-acetyl-3,5-diamino-1*H*-1,2,4-triazole). **1H NMR** ([D₆]DMSO, 25 °C): δ = 7.35 (s, 2 H, NH₂), 5.64 (s, 2 H, NH₂), 2.33 (s, 3 H, CH₃). **13C NMR** ([D₆]DMSO, 25 °C): δ = 170.5 (C=O), 162.2, 157.0, 23.6 (CH₃). **IR** (ATR, 25 °C): ν = 3414 (m), 3388 (vs), 3295 (m), 3127 (s), 1709 (s), 1640 (vs), 1568 (s), 1448 (m), 1393 (s), 1365 (vs), 1336 (s), 1178 (m), 1116 (m), 1066 (m), 1043 (m), 973 (m), 839 (w), 757 (w), 699 (w), 669 (w) cm⁻¹. **Raman** (200 mW, 25 °C): 3418(4), 3403(5), 3220(10), 3183(9), 3132(9), 3022(35), 2989(16), 2934(68), 1711(100), 1641(40), 1568(44), 1549(25), 1459(9), 1425(21), 1396(41), 1375(39), 1340(43), 1182(37), 1155(80), 1118(25), 1037(42), 972(21), 840(25), 767(8), 719(11), 668(49), 590(15), 577(17), 445(50), 399(15), 385(15), 345(39), 245(13), 224(18) cm⁻¹.

3-Acetylmino-5-amino-1*H*-1,2,4-triazole (2): A mixture of 1-acetyl-3,5-diamino-1,2,4-triazole (**1**) (10.0 g, 70.9 mmol) and decalin (100 mL) was heated to reflux without stirring at 187–190 °C for 6 h. The solid was filtered off, washed with petroleum ether (100 mL) and diethyl ether (100 mL) and dried in air to yield **2** as a colorless powder (9.6 g, 68.0 mmol, 96 %). **1H NMR** (D₂O, NaOH, 25 °C): δ = 2.03 (s, 3 H, CH₃). **13C NMR** ([D₂O, NaOH, 25 °C]): δ = 174.1 (C=O), 162.5 (C–NH₂), 154.1 (C–NHAc), 22.7 (CH₃). **IR** (ATR, 25 °C): ν = 3426 (m), 3251 (s), 1682 (vs), 1597 (vs), 1581 (vs), 1451 (s), 1295 (m), 1269 (m), 1080 (m), 1026 (w), 1010 (w), 816 (w), 714 (m) cm⁻¹. **Raman** (200 mW, 25 °C): 3243(5), 2933(39), 1684(100), 1647(12), 1586(52), 1537(11), 1456(13), 1366(24), 1296(10), 1261(8), 1084(47), 1027(45), 970(28), 818(11), 793(12), 694(4), 590(38), 493(12), 363(12), 324(24) cm⁻¹. Elemental analysis C₄H₇N₅O: calcd: C 34.04, H 5.00, N 49.62 %; found: C 34.11, H 4.86, N 49.12 %.

5,5'-Diamino-3,3'-azo-1*H*-1,2,4-triazole (3): Potassium permanganate (2/3 equiv., 1.54 g, 9.7 mmol) was added over a period of 10 minutes to a solution of 3-acetylmino-5-amino-1*H*-1,2,4-triazole (**2**,

2.0 g, 14.2 mmol) in sodium hydroxide (32 %, 15 mL) at 0 °C. The mixture was allowed to warm to room temperature and subsequently heated to reflux for 3 h after addition of sodium hydroxide (5 mL, 2 M). The generated manganese oxide was removed by filtration and the filtrate acidified with concentrated hydrochloric acid to pH = 6. The precipitate was filtered off and 5,5'-diamino-3,3'-azotriazole (**3**) was obtained as an orange solid (0.93 g, 4.8 mmol, 68 %). **13C NMR** (D₂O, NaOH): δ = 170.2 (C=N=N), 165.3 (C–NH₂). **IR** (ATR, 25 °C): ν = 3452 (s), 3351 (s), 2677 (m), 1624 (vs), 1490 (m), 1465 (m), 1413 (w), 1349 (m), 1142 (m), 1102 (m), 1051 (m), 880 (w), 799 (w), 759 (w), 708 (vw), 676 (vw) cm⁻¹. **Raman** (200 mW, 25 °C): 3349(1), 1658(2), 1520(4), 1448(42), 1388(24), 1347(100), 1139(35), 1103(7), 1056(9), 927(2), 912(3) cm⁻¹. Elemental analysis C₄H₁₀N₁₀O₂ dihydrate: calcd: C 20.87, H 4.38, N 60.85 %; found: C 21.58, H 3.85, N 59.05 %.

5,5'-Dinitrimino-3,3'-azo-1*H*-1,2,4-triazole (4): 5,5'-Diamino-3,3'-azotriazole (0.35 g, 1.8 mmol) was dissolved in sulfuric acid (conc., 1.75 mL) and nitric acid (conc., 0.30 mL, 7.2 mmol) was added at 0 °C. After stirring at 0 °C for 30 minutes, the mixture was allowed to warm to room temperature, stirred for 1 h and poured on ice (10 g). The precipitate was filtered off, washed with water, and dried at 60 °C to obtain **4** as a yellow solid. **DSC** (Onset, 5 °C·min⁻¹): T_{Dec} = 209 °C. **13C{¹H} NMR** ([D₆]DMSO, 25 °C): δ = 159.7 (C=N=N), 153.8 (C–N–NO₂). **14N NMR** ([D₆]DMSO, 25 °C): δ = -19 (NO₂). **IR** (ATR, 25 °C): ν = 3066 (s), 1695 (w), 1586 (vs), 1542 (m), 1522 (s), 1493 (m), 1436 (m), 1273 (s), 1238 (s), 1139 (m), 1075 (m), 1039 (m), 979 (m), 845 (w), 770 (w), 721 (w) cm⁻¹. **Raman** (200 mW, 25 °C): 1538(16), 1493(10), 1436(100), 1354(11), 1307(16), 1145(21), 1091(7), 994(11), 905(4), 847(3), 754(2) cm⁻¹. Elemental analysis C₄H₄N₁₂O₄: calcd: C 16.91, H 1.42, N 59.15 %; found: C 18.27, H 1.83, N 58.25 %. **Sensitivities** (grain size: 100–500 μm): FS: 20 N, IS: 2 J, ESD: 0.1 J.

General Synthesis of Nitrogen-rich Salts of DNAAT: The free nitrogen-rich base (2 equiv., 22.8 mmol) was added to a suspension of 5,5'-dinitrimino-3,3'-azo-1*H*-1,2,4-bistriazole (**4**, 3.24 g, 11.4 mmol) in water (75 mL) at 60 °C. After cooling to 5 °C, the precipitate was filtered off, washed with cold water and dried at 60 °C to yield the corresponding nitrogen-rich salt of 5,5'-dinitrimino-3,3'-azo-1*H*-1,2,4-triazole (**5–9**) as a yellow solid.

(NH₄)₂ DNAAT (5): Yield 50 %; **DSC** (onset, 5 °C·min⁻¹): T_{Dec} = 212 °C, 257 °C. **1H NMR** ([D₆]DMSO, 25 °C): δ = 13.58 (s, 2 H, N_{ring}–H), 7.23 (NH₄⁺). **13C NMR** ([D₆]DMSO, 25 °C): δ = 167.7 (C=N=N), 158.3 (C=N–NO₂). **14N NMR** ([D₆]DMSO, 25 °C): δ = -14 (-NO₂), -359 (NH₄⁺). **IR** (ATR, 25 °C): ν = 3171 (s), 1692 (w), 1641 (w), 1594 (m), 1530 (s), 1474 (s), 1432 (s), 1380 (s), 1316 (vs), 1168 (m), 1078 (s), 1035 (w), 1004 (m), 861 (w), 770 (m), 733 (w) 698 (w) cm⁻¹. **Raman** (200 mW, 25 °C): 1544(25), 1466(100), 1403(53), 1352(84), 1167(30), 1099(17), 1044(8), 1002(41), 924(12), 860(8), 748(6), 397(7) cm⁻¹. **Sensitivities** (grain size: 100–500 μm): FS: >360 N, IS: >40 J, ESD: 0.15 J.

(N₂H₅)₂ DNAAT (6): Yield 54 %. **DSC** (onset, 5 °C·min⁻¹): T_{Dec} = 154 °C, 228 °C. **1H NMR** ([D₆]DMSO, 25 °C): δ = 13.51 (s, 2 H, N_{ring}–H), 7.28 (N₂H₅⁺). **13C NMR** ([D₆]DMSO, 25 °C): δ = 166.9 (C=N=N), 157.8 (C=N–NO₂). **14N NMR** ([D₆]DMSO, 25 °C): δ = -16 (-NO₂), -359 (N₂H₅⁺). **IR** (ATR, 25 °C): ν = 3103 (s), 1631 (m), 1528 (s), 1472 (m), 1426 (s), 1385 (m), 1315 (vs), 1260 (s), 1168 (m), 1080 (s), 996 (m), 859 (w), 769 (w), 732 (vw), 705 (w) cm⁻¹. **Raman** (200 mW, 25 °C): 1541(9), 1461(100), 1403(36), 1353(54), 1258(3), 1162(19), 1100(10), 1000(20), 924(7), 859(4), 747(2), 399(2) cm⁻¹.

Sensitivities (grain size: 100–500 µm): FS: >360 N, IS: 10 J, ESD: 0.05 J.

G₂ DNAAT (7): Yield 73 %. **DSC** (onset, 5 °C·min⁻¹): $T_{\text{Dec}} = 261$ °C. **¹H NMR** ([D₆]DMSO, 25 °C): $\delta = 13.53$ (s, 2 H, N_{ring}—H), 7.03 (s, G⁺). **¹³C NMR** ([D₆]DMSO, 25 °C): $\delta = 167.1$ (C=N=N), 157.9 (C—N—NO₂), 157.7 (G⁺). **¹⁴N NMR** ([D₆]DMSO, 25 °C): $\delta = -14$ (—NO₂). **IR** (ATR, 25 °C): $\tilde{\nu} = 3336$ (m), 3241 (m), 3167 (m), 2790 (w), 1680 (m), 1635 (s), 1532 (m), 1471 (m), 1436 (m), 1391 (m), 1368 (m), 1339 (vs), 1255 (m), 1162 (m), 1085 (s), 1011 (m), 864 (w), 770 (m), 726 (w), 690 (w) cm⁻¹. **Raman** (200 mW, 25 °C): 1536(14), 1462(100), 1402(23), 1363(56), 1156(18), 1097(14), 1012(24), 917(8), 862(5), 402(5) cm⁻¹. Elemental analysis C₆H₁₄N₁₈O₄: calcd: C 17.91, H 3.51, N 62.67 %; found C 18.49, H 3.59, N 62.12 %. **Sensitivities** (grain size: 100–500 µm): FS: >360 N, IS: >40 J, ESD: 0.35 J.

AG₂ DNAAT (8): Yield 87 %. **DSC** (onset, 5 °C·min⁻¹): $T_{\text{Dec}} = 177$ °C. **¹H NMR** ([D₆]DMSO, 25 °C): $\delta = 13.61$ (s, 2 H, N_{ring}—H), 7.89 (s, AG⁺), 7.12 (s, AG⁺), 4.71 (s, AG⁺). **¹³C NMR** ([D₆]DMSO, 25 °C): $\delta = 167.0$ (C=N=N), 157.7 (C—N—NO₂), 158.9 (AG⁺). **¹⁴N NMR** ([D₆]DMSO, 25 °C): $\delta = -15$ (—NO₂). **IR** (ATR, 25 °C): $\tilde{\nu} = 3435$ (m), 3341 (m), 3252 (vs), 3183 (s), 2888 (w), 1685 (vs), 1668 (vs), 1530 (s), 1475 (m), 1436 (m), 1386 (m), 1346 (vs), 1257 (m), 1164 (w), 1086 (s), 1009 (m), 864 (w), 770 (m), 730 (w), 692 (w) cm⁻¹. **Raman** (200 mW, 25 °C): 1534(16), 1488(12), 1463(100), 1409(22), 1367(51), 1156(20), 1096(12), 1041(5), 1008(29), 918(9), 861(5), 746(4), 403(5) cm⁻¹. Elemental analysis C₆H₁₆N₂₀O₄: calcd.: C 16.67, H 3.73, N 64.80 %; found: C 16.87, H 3.73, N 61.97 %. **Sensitivities** (grain size: 100–500 µm): FS: >360 N, IS: >40 J, ESD: 0.20 J.

TAG₂ DNAAT (9): Yield 85 %. **DSC** (onset, 5 °C·min⁻¹): $T_{\text{Dec}} = 219$ °C. **¹H NMR** ([D₆]DMSO, 25 °C): $\delta = 13.48$ (s, 2 H, N_{ring}—H), 8.59 (s, TAG⁺), 4.49 (s, TAG⁺). **¹³C NMR** ([D₆]DMSO, 25 °C): $\delta = 167.3$ (C=N=N), 157.8 (C—N—NO₂), 159.0 (TAG⁺). **¹⁴N NMR** ([D₆]DMSO, 25 °C): $\delta = -14$ (—NO₂). **IR** (ATR, 25 °C): $\tilde{\nu} = 3252$ (s), 1682 (s), 1526 (s), 1466 (m), 1435 (s), 1315 (vs), 1250 (m), 1133 (m), 1073 (s), 1003 (m), 857 (w), 771 (w), 728 (w), 656 (w) cm⁻¹. **Raman** (200 mW, 25 °C): 1534(16), 1488(12), 1463(100), 1409(22), 1367(51), 1156(20), 1096(12), 1041(5), 1008(29), 918(9), 861(5), 746(4), 403(5) cm⁻¹. Elemental analysis C₆H₂₀N₂₄O₄: calcd.: C 14.64, H 4.09, N 68.27 %; found: C 15.22, H 4.37, N 66.73 %. **Sensitivities** (grain size: 100–500 µm): FS: 160 N, IS: >40 J, ESD: 0.20 J.

Acknowledgement

Financial support of this work by the *Ludwig-Maximilian University of Munich* (LMU), the *U.S. Army Research Laboratory* (ARL), the *Armament Research, Development and Engineering Center* (ARDEC), the *Strategic Environmental Research and Development Program* (SERDP), and the *Office of Naval Research* (ONR Global, title: “Synthesis and Characterization of New High Energy Dense Oxidizers (HEDO) - NICOP Effort”) under contract nos. W911NF-09-2-0018 (ARL), W911NF-09-1-0120 (ARDEC), W011NF-09-1-0056 (ARDEC), and 10 WPSEED01-002 / WP-1765 (SERDP) is gratefully acknowledged. The authors acknowledge collaborations with *Dr. Mila Krupka* (OZM Research, Czech Republic) in the development of new testing and evaluation methods for energetic materials and with *Dr. Muhamed Sucesca* (Brodarski Institute, Croatia) in the development of new computational codes to predict the detonation and propulsion parameters of novel explosives. We are indebted to and thank *Drs. Betsy M. Rice* and *Brad Forch* (ARL, Aberdeen, Proving Ground, MD) and *Mr. Gary Chen* (ARDEC, Picatinny Arsenal, NJ) for many helpful

and inspired discussions and support of our work. We are also indebted to and thank *Dr. Jörg Stierstorfer* for performing quantum mechanical and performance calculations.

References

- P. F. Pagoria, G. S. Lee, A. R. Mitchell, R. D. Schmidt, *Thermochim. Acta* **2002**, *384*, 187–204.
- T. M. Klapötke, in: *Structure and Bonding* (Ed.: D. M. P. Mingos), Springer-Verlag, Berlin Heidelberg, Germany **2007**.
- D. Fournier, A. Halasz, J. Spain, R. J. Spanggord, J. C. Bottaro, J. Hawari, *Appl. Environ. Microbiol.* **2004**, *70*, 1123–1128.
- a) T. M. Klapötke, J. Stierstorfer, A. U. Wallek, *Chem. Mater.* **2008**, *20*, 4519–4530; b) T. M. Klapötke, C. M. Sabate, *Chem. Mater.* **2008**, *20*, 3629–3637; c) S. Yang, S. Xu, H. Huang, W. Zhang, X. Zhang, *Huaxue* **2008**, *20*, 526–537; d) D. E. Chavez, M. A. Hiskey, D. L. Naud, *Propellants, Explos., Pyrotech.* **2004**, *29*, 209–215; e) Y. Huang, H. Gao, B. Twamley, J. N. M. Shreeve, *Eur. J. Inorg. Chem.* **2008**, 2560–2568.
- C. M. Sabate, T. M. Klapötke, *New Trends in Research of Energetic Materials*, Proceedings of the Seminar, 12th, Pardubice, Czech Republic, Apr. 1–3, **2009**, 172–194.
- a) D. E. Chavez, M. A. Hiskey, R. D. Gilardi, *Angew. Chem. Int. Ed.* **2000**, *39*, 1791–1793; b) D. Chavez, L. Hill, M. Hiskey, S. Kinkead, *J. Energ. Mater.* **2000**, *18*, 219–236.
- a) T. M. Klapötke, C. M. Sabate, *New J. Chem.* **2009**, *33*, 1605–1617; b) T. M. Klapötke, C. M. Sabate, *Chem. Mater.* **2008**, *20*, 1750–1763; c) A. Hammerl, G. Holl, T. M. Klapötke, P. Mayer, H. Noth, H. Piotrowski, M. Warchhold, *Eur. J. Inorg. Chem.* **2002**, 834–845.
- a) B. C. Tappan, A. N. Ali, S. F. Son, T. B. Brill, *Propellants, Explos., Pyrotech.* **2006**, *31*, 163–168; b) R. Sivabalan, M. B. Talawar, N. Senthilkumar, B. Kavitha, S. N. Asthana, *J. Therm. Anal. Calorim.* **2004**, *78*, 781–792.
- M. A. Hiskey, N. Goldman, J. R. Stine, *J. Energ. Mater.* **1998**, *16*, 119–127.
- a) M. M. Chaudhri, *J. Mater. Sci. Lett.* **1984**, *3*, 565–568; b) D. J. Whelan, R. J. Spear, R. W. Read, *Thermochim. Acta* **1984**, *80*, 149–163; c) G. O. Reddy, A. K. Chatterjee, *Thermochim. Acta* **1983**, *66*, 231–244; d) M. M. Chaudhri, *Nature* **1976**, *263*, 121–122.
- M. M. Williams, W. S. McEwan, R. A. Henry, *J. Phys. Chem.* **1957**, *61*, 261–267.
- D. E. Chavez, B. C. Tappan, *8-ISICP*, Los Alamos National Laboratory, **2009**.
- D. L. Naud, M. A. Hiskey, H. H. Harry, *J. Energ. Mater.* **2003**, *21*, 57–62.
- D. E. Chavez, B. C. Tappan, B. A. Mason, D. Parrish, *Propellants, Explos., Pyrotech.* **2009**, *34*, 475–479.
- B. G. van den Bos, *Rec. Trav. Chim. Pays-Bas Belgique* **1960**, *79*, 836–842.
- M. S. Pevzner, N. V. Gladkova, T. A. Kravchenko, *Zh. Org. Khim.* **1996**, *32*, 1230–1233.
- H.-H. Licht, H. Ritter, *J. Energ. Mater.* **1994**, *12*, 223–235.
- N. Biswas, S. Umapathy, *J. Phys. Chem. A* **2000**, *104*, 2734–2745.
- F. Billes, H. Endredi, G. Kereszty, *THEOCHEM* **2000**, *530*, 183–200.
- CrysAlis CCD*, Oxford Diffraction Ltd., Version 1.171.27p5 beta (release 01-04-2005 CrysAlis171.NET), **2005**.
- CrysAlis RED*, Oxford Diffraction Ltd., Version 1.171.27p5 beta (release 01-04-2005 CrysAlis171.NET), **2005**.
- A. Altomare, G. Cascarano, C. Giacovazzo, A. Guagliardi, *J. Appl. Crystallogr.* **1993**, *26*, 343–350.
- G. M. Sheldrick, *SHELXS-97*, Program for Crystal Structure Solution, University of Göttingen, Germany, **1990**.
- G. M. Sheldrick, *SHELXL-97*, Program for the Refinement of Crystal Structures, University of Göttingen, Germany, **1997**.
- L. Farrugia, *J. Appl. Crystallogr.* **1999**, *32*, 837–838.

- [26] A. L. Spek, *Platon, A Multipurpose Crystallographic Tool*, Utrecht University, Utrecht, The Netherlands, **1999**.
- [27] Crystallographic data for the structures in this paper have been deposited with the Cambridge Crystallographic Data Centre as supplementary publication nos. CCDC-807480 (**4·DMSO**), -807481 (**4·THF**), -807482 (**5**) and -807483 (**9**). Copies of the data can be obtained free of charge on application to The Director, CCDC, 12 Union Road, Cambridge CB2 1EZ, UK (Fax: 44-1223-336-033; E-Mail for inquiry: fileserv@ccdc.cam.ac.uk; E-Mail for deposition: deposit@ccdc.cam.ac.uk).
- [28] F. H. Allen, O. Kennard, D. G. Watson, L. Brammer, A. G. Orpen, R. Taylor, *J. Chem. Soc. Perk. Trans. 2*, **1987**, S1–S19.
- [29] A. Hammerl, Ludwig-Maximilians-University, Munich **2001**.
- [30] G. A. Jeffrey, *An Introduction to Hydrogen Bonding*, Oxford University Press, Oxford **1997**.
- [31] A. F. Holleman, E. Wiberg, N. Wiberg, *Lehrbuch der Anorganischen Chemie*, de Gruyter, New York, **2007**.
- [32] M. J. Frisch, G. W. Trucks, H. B. Schlegel, G. E. Scuseria, M. A. Robb, J. R. Cheeseman, J. A. Montgomery, Jr., T. Vreven, K. N. Kudin, J. C. Burant, J. M. Millam, S. S. Iyengar, J. Tomasi, V. Barone, B. Mennucci, M. Cossi, G. Scalmani, N. Rega, G. A. Petersson, H. Nakatsuji, M. Hada, M. Ehara, K. Toyota, R. Fukuda, J. Hasegawa, M. Ishida, T. Nakajima, Y. Honda, O. Kitao, H. Nakai, M. Klene, X. Li, J. E. Knox, H. P. Hratchian, J. B. Cross, V. Bakken, C. Adamo, J. Jaramillo, R. Gomperts, R. E. Stratmann, O. Yazyev, A. J. Austin, R. Cammi, C. Pomelli, J. W. Ochterski, P. Y. Ayala, K. Morokuma, G. A. Voth, P. Salvador, J. J. Dannenberg, V. G. Zakrzewski, S. Dapprich, A. D. Daniels, M. C. Strain, O. Farkas, D. K. Malick, A. D. Rabuck, K. Raghavachari, J. B. Foresman, J. V. Ortiz, Q. Cui, A. G. Baboul, S. Clifford, J. Cioslowski, B. B. Stefanov, G. Liu, A. Liashenko, P. Piskorz, I. Komaromi, R. L. Martin, D. J. Fox, T. Keith, M. A. Al-Laham, C. Y. Peng, A. Nanayakkara, M. Challacombe, P. M. W. Gill, B. Johnson, W. Chen, M. W. Wong, C. Gonzalez, J. A. Pople, *Gaussian 03*, Revision B04, Gaussian Inc., Wallingford, CT, **2004**.
- [33] a) J. W. Ochterski, G. A. Petersson, J. A. Montgomery Jr., *J. Chem. Phys.* **1996**, *104*, 2598–2619; b) J. A. Montgomery Jr., M. J. Frisch, J. W. Ochterski, G. A. Petersson, *J. Chem. Phys.* **2000**, *112*, 6532–6542.
- [34] a) L. A. Curtiss, K. Raghavachari, P. C. Redfern, J. A. Pople, *J. Chem. Phys.* **1997**, *106*, 1063–1079; b) E. F. C. Byrd, B. M. Rice, *J. Phys. Chem. A* **2006**, *110*, 1005–1013; c) B. M. Rice, S. V. Pai, J. Hare, *Combust. Flame* **1999**, *118*, 445–458.
- [35] <http://webbook.nist.gov/chemistry>.
- [36] a) M. S. Westwell, M. S. Searle, D. J. Wales, D. H. Williams, *J. Am. Chem. Soc.* **1995**, *117*, 5013–5015; b) F. Trouton, *Philos. Mag.* **1884**, *18*, 54–57.
- [37] a) H. D. B. Jenkins, H. K. Roobottom, J. Passmore, L. Glasser, *Inorg. Chem.* **1999**, *38*, 3609–3620; b) H. D. B. Jenkins, D. Tudela, L. Glasser, *Inorg. Chem.* **2002**, *41*, 2364–2367.
- [38] a) M. Sućeska, *EXPLO5.4* program, Zagreb, Croatia, **2010**; b) M. Sućeska, *EXPLO5.3* program, Zagreb, Croatia, **2009**.
- [39] a) M. Sućeska, *Mater. Sci. Forum* **2004**, *465–466*, 325–330; b) M. Sućeska, *Propellants, Explos., Pyrotech.* **1991**, *16*, 197–202; c) M. Sućeska, *Propellants, Explos., Pyrotech.* **1999**, *24*, 280–285; d) M. L. Hobbs, M. R. Baer, in: *Proc. of the 10th Symp. (International) on Detonation*, ONR 33395–12, Boston, MA, July 12–16, **1993**, p. 409.
- [40] Calculation of oxygen balance: $\Omega (\%) = (wO - 2xC - 1/2yH - 2zS)1600/M$. (w: number of oxygen atoms, x: number of carbon atoms, y: number of hydrogen atoms, z: number of sulfur atoms, M: molecular weight).
- [41] J. Köhler, R. Meyer, *Explosivstoffe*, 9th ed., Wiley-VCH, Weinheim, Germany **1998**.
- [42] *NATO standardization agreement (STANAG) on explosives*, no.4489, 1st ed., Sept. 17, **1999**.
- [43] *WIWEB-Standardarbeitsanweisung 4–5.1.02*, Ermittlung der Explosionsgefährlichkeit, hier: der Schlagempfindlichkeit mit dem Fallhammer, Nov. 08, **2002**.
- [44] <http://www.bam.de>.
- [45] *NATO standardization agreement (STANAG) on explosives, friction tests*, no.4487, 1st ed., Aug. 22, **2002**.
- [46] *WIWEB-Standardarbeitsanweisung 4–5.1.03*, Ermittlung der Explosionsgefährlichkeit, hier: der Reibempfindlichkeit mit dem Reibeapparat, Nov. 08, **2002**.
- [47] *NATO standardization agreement (STANAG) on explosives, electrostatic discharge sensitivity tests*, no.4490, 1st ed., Feb. 19, **2001**.

Received: March 2, 2011
Published Online: May 5, 2011